In vitro Cytotoxicity of Activated Carbon from *Musa Acuminate* Fruit Peel Against HepG-2 Cells

Shanmugasundaram M [1*], Prasath S [2], Geetha N B [2], Manikandan S [2]

Abstract

Background: Cancer is a leading cause of global mortality, necessitating the development of new therapeutic options. Plant-based medicines offer advantages over conventional drugs, prompting investigations into their cytotoxic potential. This study aimed to evaluate the cytotoxicity of activated carbon derived from M. acuminate fruit peel against HepG-2 cells. Methods: Activated carbon was prepared from M. acuminate fruit peel, and its cytotoxic effects were assessed using MTT assay, DAPI/PI/EtBr staining, and comet assay. Statistical analyses were conducted to evaluate significance. Results: Dose-dependent cytotoxicity was observed, with a notable reduction in cell viability with approximately 50% cytotoxicity observed at a concentration of 86.74 µg/ml after 48 hours. Activated carbon significantly increased reactive oxygen species (ROS) synthesis, mitochondrial membrane potential attenuation, induction of apoptotic morphology, and caspase-3 activation in HepG-2 cells. Conclusion: The study demonstrates the potential of activated carbon as a natural product source for developing novel cancer medicines. Its cytotoxic effects against HepG-2 cells, mediated via ROS-mediated mitochondrial pathway and caspase-3 activation, warrant further investigation for therapeutic applications.

Keywords: *Musa Acuminate*, HepG-2 cells, MTT, DAPI/PI/EtBr staining and comet assay.

Significance | Activated carbon from *Musa Acuminate* exhibits potent inhibitory effects on HepG-2 cells via ROS-mediated MTD pathway, suggesting therapeutic potential against cancer.

*Correspondence. Shanmugasundaram M, Mohamed Sathak AJ College of Engineering, Chennai 603103
E-mail: headprojects@msajce-edu.in

Editor Mohamed Khadeer Ahamed Basheer And accepted by the Editorial Board Feb 25, 2024 (received for review Dec 25, 2023)

Introduction

Activated carbon, treated to enhance surface area, is used for detoxification, particularly in poisoning cases, effectively absorbing various drugs (Wu et al., 2013; Qureshi et al., 2008; Chen et al., 2011; Foo & Hameed, 2012; Njoku et al., 2014; Njoku et al., 2015; Rahman & Chin, 2019). Rapid absorption, within an hour, is noted (Lakshmi et al., 2018). Effective against acetaminophen, lanoxin, digitoxin, tricyclic antidepressants, and phenobarbital poisoning in adults and children (González-García, 2018; Gupta et al., 2016). However, ineffective against strong acids or bases, cyanides, ethanol, methanol, iron, lithium, etc. (Elanthamilan et al., 2019; Nanda et al., 2016). Often administered with laxatives, although support for this combination is lacking (Galan et al., 2018; Wang et al., 2020; Zare et al., 2015), potentially causing adverse effects (Spessato et al., 2019).

Activated carbon shows promise in treating gastrointestinal issues like diarrhea, gas, and indigestion, including chemotherapy-induced diarrhea (Rawal et al., 2018). It aids in reducing bloating and stomach stress, enhancing the effects of indigestion when combined with simethicone (Rahimian & Zarinabadi, 2020). Furthermore, it has potential applications in treating hepatitis and renal disturbances due to its adsorption properties (Gupta et al., 2021). Oral intake of activated carbon can also lower cholesterol and bile acid levels (Dulyaseree et al., 2017). Additionally, light

Author Affiliation.
[1] Mohamed Sathak AJ College of Engineering, Chennai 603103
[2] Dhaanish Ahmed College of Engineering, Chennai 601301

Please cite this article.
Shanmugasundaram M, Prasath S, Geetha N B T et al., (2024). In vitro Cytotoxicity of Activated Carbon from Musa Acuminate Fruit Peel Against HepG-2 Cells, Journal of Angiotherapy, 8(2), 1-6, 9527

therapy with activated carbon can prevent jaundice in newborns (Beck et al., 2017). Activated carbon particles are being studied for their potential in drug delivery to improve therapy and minimize side effects (Sharifpour et al., 2018). However, further research is needed to fully understand its mechanisms and potential applications.

Materials and methods

Preparation of Activated Carbon

Activated Carbon from ***Musa Acuminate*** fruit peel was prepared following the method by Ashok and Babu (2020). ***Musa Acuminate*** (Banana) peels were cut into approximately 3 cm pieces, which were then dried in an oven. Once dried, the peels underwent carbonization in a furnace (Line Thermocline FB1410M-33) at 400°C for 1.5 hours. The resulting carbon was crushed and passed through 100-mesh sieves for uniformity. Chemical activation was performed using potassium hydroxide (KOH) solutions of varying concentrations (1, 2, and 3 N) for different durations (1, 2, and 3 hours, respectively). The activated carbon was then filtered and washed until it reached a neutral pH, followed by heating at 200°C for 2 hours. The produced banana peel activated carbon (BPAC) was mixed with adhesive and shaped into cubes measuring 1 cm in length, width, and height. After solidification, the BPAC cubes were further heated in an oven at 120°C for 3 hours.

MTT assay

HepG-2 and Vero cells were cultured following Mosmann's MTT method (1983) to test cell viability. HepG-2 cells were seeded at 7 x 10^3 cells/well in a 96-well plate and incubated overnight at 37°C with 5% CO2. After reaching full confluence, cells were exposed to various concentrations of solvent-extracted material (25-125 µg/ml) for 24 and 48 hours. Then, 50 µl of MTT solution (5 mg/ml) was added to each well and incubated for 3 hours. After discarding the contents, the plate was dried overnight at room temperature. Purple formazone crystals were dissolved by shaking in 100 µl of DMSO for 15 minutes. The absorbance of the solution was measured at 570 nm using a microplate reader to determine cell viability percentage. Analysis, including growth percentage, percentage inhibition, and IC50, was conducted using a pre-programmed MS-Excel prototype.

$$\text{Cell viability \%} = \frac{OD\ sample\ x100}{OD\ control}$$

DAPI/PI/EtBr staining

Cells were stained with nuclear dyes to assess apoptotic cell morphology following the method of Spector et al. (2001). HepG-2 cells at full confluence were trypsinized and seeded onto 22 x 22 mm coverslips in 6-well plates at a density of 1 x 10^5 cells per cover slip. After overnight incubation in a CO2 incubator at 37°C with 5% CO2, cells were exposed to ACTIVATED CARBON at IC50 levels for 24 hours under controlled humidified conditions. After incubation, cells were washed with 1X PBS, stained with 50 µl of PI, and incubated in the dark at room temperature for 20 minutes. Following another PBS wash, cells were stained with 50 µl of DAPI/PI/EtBr and immediately washed with 1X PBS. Cover slips were transferred to new slides and examined under a fluorescence microscope (20X magnification, Carl Zeiss) to capture cell images from various fields.

Comet Assay/SCGE

SCGE was performed following Singh et al. (1988) to assess DNA stability and damage in HepG-2 cells. Slides were electrophoresed horizontally, submerged in buffer, and run for 15 minutes at 0.8 Volts/cm. After neutralization and staining with DAPI, DNA migration was analyzed under a fluorescence microscope at 200X magnification using CASPLab (1.2.3 beta2).

Statistical Analysis

Two-Way ANOVA analysed the data to evaluate the importance between the control and experimental classes. Statistical importance was taken into consideration at $p < 0.05$.

Results and Discussion

Activated carbon, characterized by its porous structure, efficiently absorbs organic particles like drugs through adsorption within its microholes. As a carrier for drugs, activated carbon exhibits unique properties in drug release. Chemicals are adsorbed onto activated carbon through physical contact rather than covalent bonding, allowing for easy release of drugs into free pharmaceutical particles upon contact with the surface. This property enables medication accumulation in targeted areas, offering significant benefits in drug delivery. Activated carbon demonstrates considerable effectiveness against HepG-2 cells, albeit potentially harmful to the environment due to its discharge. Its effects range from 0.8 to 200 µg/ml, with released chemical molecules temporarily encapsulated around carrier particles, facilitating localized drug accumulation. With smaller diameter and larger surface area, activated carbon enhances drug adsorption and transport, ensuring minimal loss during administration to medicinal sites.

The impact of activated carbon was assessed using the MTT method on HepG-2 CA cell lines at 25, 50, 75, 100, and 125 µg/ml concentrations. Results showed a dose-dependent decrease in cell viability (CV) and cytotoxicity (CYT) with prolonged incubation. At 86.74 µg/ml for 48 hours, approximately 50% CYT inhibition was observed, but IC50 values were not achieved within 48 hours (Figure 1, 2).

Significant improvements in nuclear morphology were observed in the fluorescence microscopy (FLMICRO) experiments. DAPI staining revealed apoptotic (APT) nuclear morphology in both control and experimental groups of HepG-2 cells. Our trial

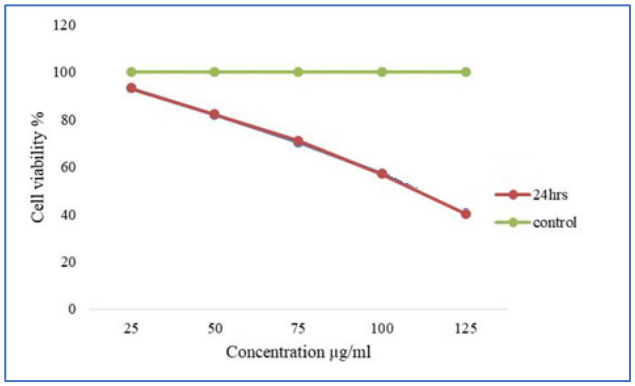

Figure 1. Per CV of HepG-2 cell when treated for 24 h various concentration of activated carbon

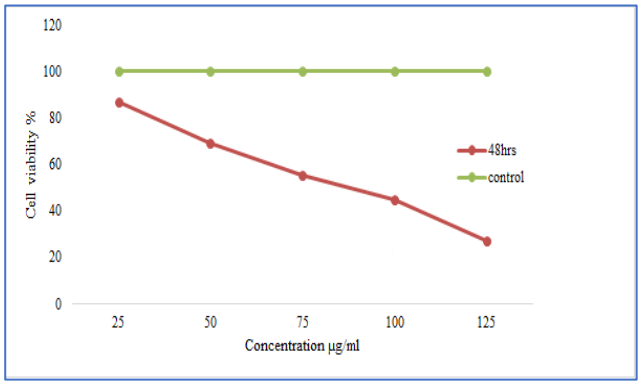

Figure 2. Per cv of hepg-2 cell when treated for 48 h various concentration of activated carbon

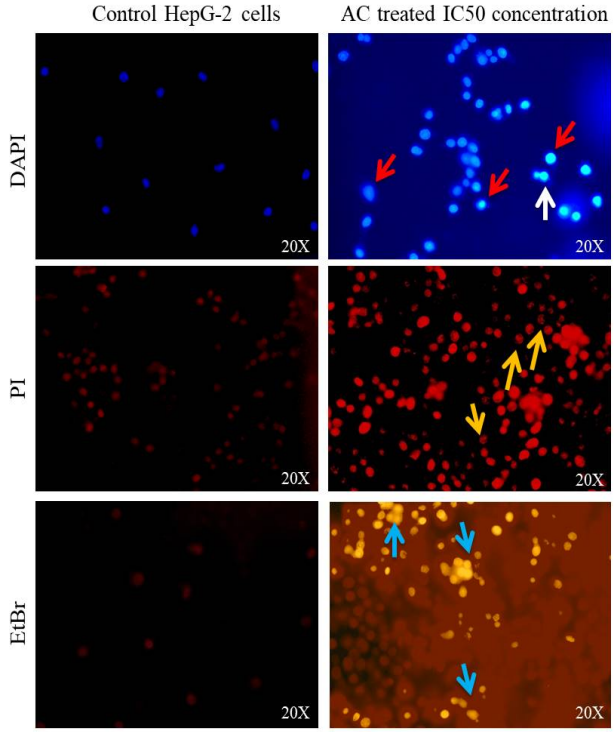

Figure 3. DAPI/PI/EtBr staining of HepG-2 cells

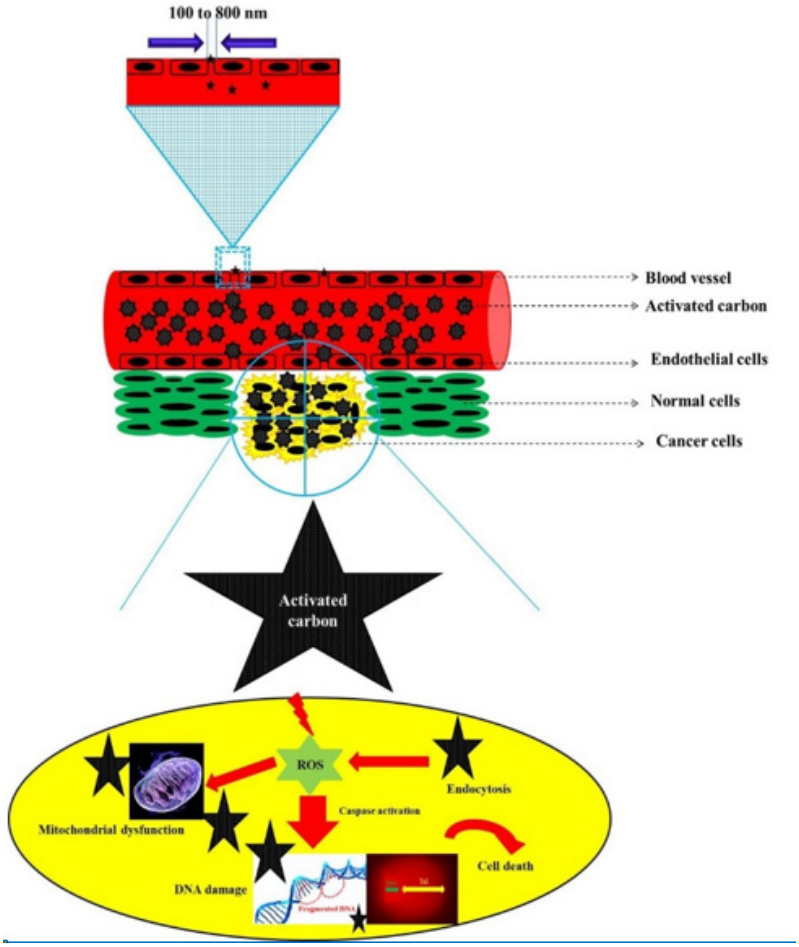

Figure 4: Anticancer mechanism of activated carbontivated carbon when treated with HepG-2 cells

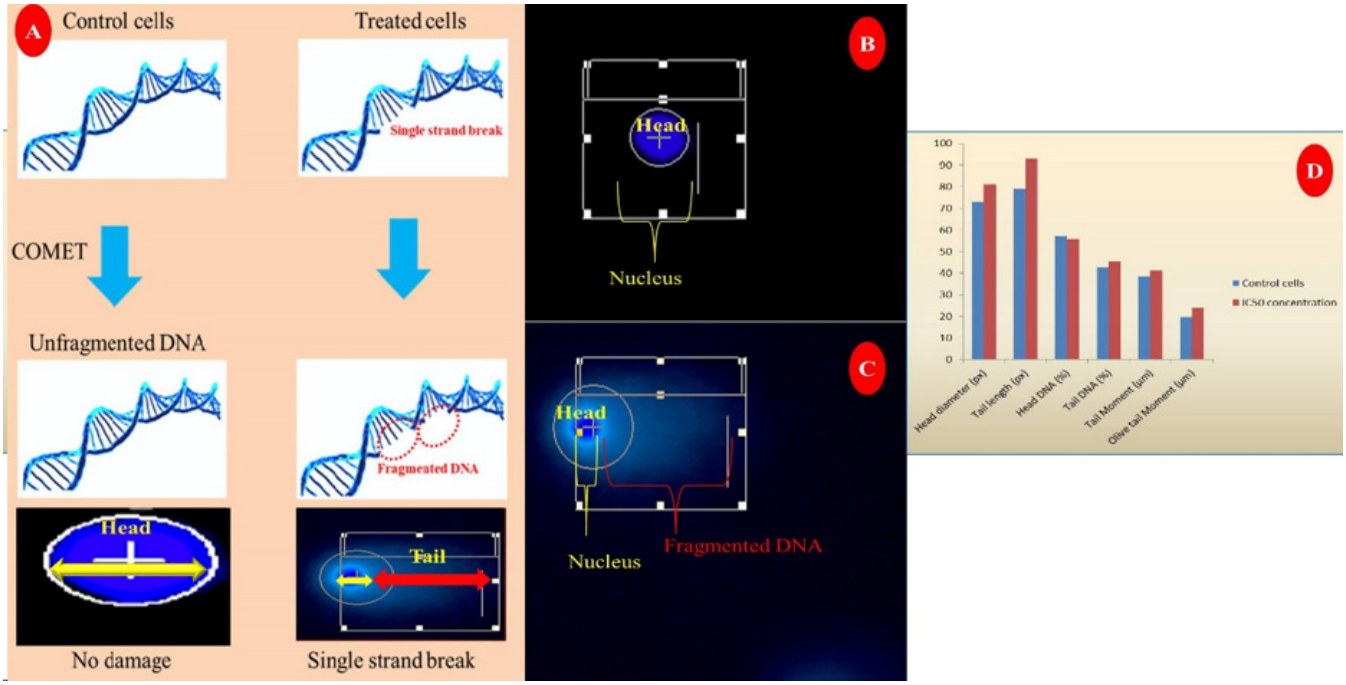

Figure 5. (A) SCGE mechanism, (B) Control (untreated) HepG-2 cells where the DNA remains intactivated carbont, (C) IC_{50} concentration of activated carbon and (D) Quantitative DNA fragmentation analysis of HepG-2 cells when treated with 48 h IC_{50} concentration of activated carbon to measure the SCGE head diameter, tail length, head DNA, tail DNA, tail moment and olive tail moment.

indicated an 80% increase in DAPI staining in HepG-2 cells undergoing apoptosis compared to the control. The potential mechanism involves activated carbon triggering the permeability of the mitochondrial outer membrane, leading to cytochrome-C release during apoptosis. This activates caspases, orchestrating cell death by disrupting mitochondrial function and generating reactive oxygen species (ROS). Activating the mitochondrial pathway may be a crucial step in apoptosis, involving recruiting Caspase family proteins such as caspase-8 and/or caspase-3 (Figure 4). ACTIVATED CARBON also exhibits cytoprotective effects, including scavenging free radicals and modulating enzymes that detoxify carcinogens.

Cytomorphological observations of HepG-2 cells using DAPI staining were conducted under fluorescence microscopy (FLMICRO). Control HepG-2 cells exhibited intact nuclei with uniform shape and size, displaying smooth edges. In contrast, HepG-2 cells treated with the IC50 concentration of ACTIVATED CARBON showed apoptotic (APT) bodies, indicated by red arrows, and disintegration or cracking of cells, as denoted by white arrows. DAPI staining revealed a concentration-dependent induction of apoptosis and cell disintegration in Activated carbon-treated cells. Yellow arrows highlight PI reticular patterns of nuclear staining, while blue arrows indicate nuclear condensation, fragmentation, and APT bodies observed in EtBr-stained cells treated with the IC50 concentration. The DAPI/PI/EtBr staining results demonstrated a higher occurrence of APT cells in the IC50 concentration treated cells compared to the control, as illustrated in Figure 3.

The Comet assay, also known as single-cell gel electrophoresis (SCGE), is a highly sensitive technique to detect and quantify even small amounts of double-strand DNA damage in individual cells. After lysing the cells to remove cytoplasmic proteins, the DNA is allowed to unwind under alkaline conditions and then subjected to electrophoresis in a gel. Damaged DNA migrates from the negative to the positive pole in the gel, forming the tail part of the comet, while intact DNA forms the head. Staining with DAPI reveals the extent of DNA damage, with blue fluorescence indicating damage in the head, tail, and tail length regions. This assay provides valuable insights into DNA damage levels in various cell types, as illustrated in Figure 5.

Conclusion

In conclusion, this study highlights the significant inhibitory effect of ACTIVATED CARBON on HepG-2 cell formation, likely mediated by the ROS-mediated MTD pathway and activated caspase-3 induction leading to APA cell death. These findings underscore the potential of ACTIVATED CARBON as a valuable natural resource for developing new CA medicines. Further research is essential to elucidate the underlying mechanisms and explore the therapeutic potential of ACTIVATED CARBON in vivo.

Author contribution

S.M., P.S., G.N.B., M.S. conceptualized, reviewed the literature, and wrote the article.

Acknowledgment

None declared

Competing financial interests

The authors have no conflict of interest.

References

Abid et al (2019). Synthesis and Charactivated carbonterization of Biochar from Peel and Seed of Jactivated carbonkfruit plant waste for the adsorption of Copper Metal Ion from water. Research Journal of Pharmactivated carbony and Technology, 12(9), 4182-4188.

Ashok and Babu (2020). Antiproliferative activated carbontivity of activated carbontivated carbon produced from Musa activated carbonuminate fruit peel against MDA-MB-231 cell line. Malaya Journal of Matematik, S(2): 4427-4429.

Beck et al (2017). Electrospun lignin carbon nanofiber membranes with large pores for highly efficient adsorptive water treatment applications. Journal of water process engineering, 16, 240-248.

Chen et al (2011). On the preparation and charactivated carbonterization of activated carbontivated carbon from mangosteen shell. Journal of the Taiwan Institute of Chemical Engineers, 42(5), 837-842.

Chu et al (2013). Laser light triggered-activated carbontivated carbon nanosystem for cancer therapy. Biomaterials, 34(7), 1820-1832.

Daniluk et al (2020). Use of Selected Carbon Nanoparticles as Melittin Carriers for MCF-7 and MDA-MB-231 Human Breast Cancer Cells. Materials, 13(1), 90.

Dulyaseree et al (2017). Nitrogen-rich green leaves of papaya and Coccinia grandis as precursors of activated carbontivated carbon and their electrochemical properties. RSC advances, 7(67), 42064-42072.

Elanthamilan et al (2019). Couroupita guianansis dead flower derived porous activated carbontivated carbon as efficient supercapactivated carbonitor electrode material. Materials Research Bulletin, 112, 390-398.

Foo & Hameed (2012). Factivated carbontors affecting the carbon yield and adsorption capability of the mangosteen peel activated carbontivated carbon prepared by microwave assisted K2CO3 activated carbontivation. Chemical Engineering Journal, 180, 66-74.

Galan et al (2018). Green synthesis of copper oxide nanoparticles impregnated on activated carbontivated carbon using Moringa oleifera leaves extractivated carbont for the removal of nitrates from water. The Canadian Journal of Chemical Engineering, 96(11), 2378-2386.

Gin et al (2014). Production of activated carbontivated carbon from watermelon peel. Int. J. Scient. Eng. Res, 5, 66-71.

González-García (2018). Activated carbontivated carbon from lignocellulosics precursors: A review of the synthesis methods, charactivated carbonterization techniques and applications. Renewable and Sustainable Energy Reviews, 82, 1393-1414.

Gotoh et al (1990). A study on cisplatin adsorbed to activated carbontivated carbon particles as a new drug delivery system and its anti-cancer effect against human bladder cancer cell lines. Nihon Hinyokika Gakkai zasshi. The japanese journal of urology, 81(9), 1337-1342.

Gupta et al (2016). Cellulose: a review as natural, modified and activated carbontivated carbon adsorbent. Bioresource technology, 216, 1066-1076.

Gupta et al (2021). A novel approactivated carbonh to develop activated carbontivated carbon by an ingenious hydrothermal treatment methodology using Phyllanthus emblica fruit stone. Journal of Cleaner Production, 288, 125643.

Hashem et al (2016). Comparative study on activated carbontivated carbon prepared from various fruit peels. International Journal of Innovative Research in Science, Engineering and Technology, 5(3), 2750-2759.

Lakshmi et al (2018). Activated carbontivated carbon nanoparticles from biowaste as new generation antimicrobial agents: A review. Nano-Structures & Nano-Objects, 16, 306-321.

Mosmann (1983). Rapid colorimetric assay for cellular growth and survival: Application to proliferation and cytotoxicity assays. J. Immunol. Methods, 65(2): 55-63.

Nanda et al (2016). Biochar as an exceptional bioresource for energy, agronomy, carbon sequestration, activated carbontivated carbon and specialty materials. Waste and Biomass Valorization, 7(2), 201-235.

Njoku et al (2014). Utilization of sky fruit husk agricultural waste to produce high quality activated carbontivated carbon for the herbicide bentazon adsorption. Chemical Engineering Journal, 251, 183-191.

Njoku et al (2015). Adsorption of 2, 4-dichlorophenoxyactivated carbonetic activated carbonid by mesoporous activated carbontivated carbon prepared from H3PO4-activated carbontivated langsat empty fruit bunch. Journal of Environmental Management, 154, 138-144.

Qureshi et al (2008). Physical and chemical analysis of activated carbontivated carbon prepared from sugarcane bagasse and use for sugar decolorisation. International Journal of Chemical and Biomolecular Engineering, 1(3), 145-149.

Rahimian & Zarinabadi (2020). A review of studies on the removal of methylene blue dye from industrial wastewater using activated carbontivated carbon adsorbents made from almond bark. Progress in Chemical and Biochemical Research, 3(3), 251-268.

Rahman & Chin (2019). Physical and chemical properties of the rice straw activated carbontivated carbon produced from carbonization and KOH activated carbontivation processes. Sains Malaysiana, 48(2), 385-391.

Rawal et al (2018). Synthesis and charactivated carbonterization of activated carbontivated carbon from the biomass of Sactivated carboncharum bengalense for electrochemical supercapactivated carbonitors. Journal of Energy Storage, 20, 418-426.

Sharifpour et al (2018). Zinc oxide nanorod-loaded activated carbontivated carbon for ultrasound-assisted adsorption of safranin O: Central composite design and genetic algorithm optimization. Applied organometallic chemistry, 32(2), e4099.

Singh et al (1988). A simple technique for quantification of low levels of DNA damage in individual cells. Exp. Cell Res., 175(1): 184-191.

Spector et al (2001). Cell culture analysis: Apoptosis analysis. In: "Cell - A Laboratory Manual". (4th ed.), (Eds.), Coldspring Harbour Laboratory Press, New York, USA. pp. 6-15.

Spessato et al (2019). KOH-super activated carbontivated carbon from biomass waste: Insights into the paractivated carbonetamol adsorption mechanism and thermal regeneration cycles. Journal of hazardous materials, 371, 499-505.

Wang et al (2020). Preparation of activated carbontivated carbon from peanut shell with KOH activated carbontivation and its application for H2S adsorption in confined spactivated carbone. Journal of Environmental Chemical Engineering, 8(2), 103683.

Wu et al (2013). Preparation and charactivated carbonteristics of medicinal activated carbontivated carbon powders by CO2 activated carbontivation of peanut shells. Powder technology, 247, 188-196.

Zare et al (2015). A comparative study on the basis of adsorption capactivated carbonity between CNTs and activated carbontivated carbon as adsorbents for removal of noxious synthetic dyes: a review. Journal of nanostructure in chemistry, 5(2), 227-236.